






RESEARCH ARTICLE

MRI and flortaucipir relationships in Alzheimer's phenotypes are heterogeneous

Keith A. Josephs¹ , Nirubol Tosakulwong², Jonathan Graff-Radford¹ , Stephen D. Weigand², Marina Buciu¹ , Mary M. Machulda³, David T. Jones¹, Christopher G. Schwarz⁴ , Matthew L. Senjem^{4,5}, Nilufer Ertekin-Taner⁶, Kejal Kantarci⁴, Bradley F. Boeve¹, David S. Knopman¹ , Clifford R. Jack Jr⁴, Ronald C. Petersen¹, Val J. Lowe⁴ & Jennifer L. Whitwell⁴

¹Department of Neurology, Mayo Clinic, Rochester, Minnesota

²Department of Health Science Research (Biostatistics), Mayo Clinic, Rochester, Minnesota

³Department of Psychiatry and Psychology, Mayo Clinic, Rochester, Minnesota

⁴Department of Radiology, Mayo Clinic, Rochester, Minnesota

⁵Department of Information Technology, Mayo Clinic, Rochester, Minnesota

⁶Department of Neuroscience (Neurogenetics), Mayo Clinic, Jacksonville, Florida

Correspondence

Keith A. Josephs, Department of Neurology, Behavioral Neurology and Movement Disorders, Mayo Clinic, College of Medicine and Science, 200 1st Street S.W., Rochester, MN 55905, USA. Tel: +1 (507) 538 1038; Fax: +1 (507) 538 6012; E-mail: josephs.keith@mayo.edu

Funding Information

NIH R01-AG50603, P50-AG16574, P30 AG062677, R01-AG11378, U01-AG006786, and the Elsie and Marvin Dekelbourn Family Foundation and the Oxley Foundation.

Received: 23 December 2019; Revised: 28 February 2020; Accepted: 16 March 2020

Annals of Clinical and Translational Neurology 2020; 7(5): 707–721

doi: 10.1002/acn3.51038

Abstract

Objective: To assess the relationships between MRI volumetry and [¹⁸F]flortaucipir PET of typical and atypical clinical phenotypes of Alzheimer's disease, by genarian (age by decade). **Methods:** Five-hundred and sixty-four participants including those with typical ($n = 86$) or atypical ($n = 80$) Alzheimer's dementia and normal controls ($n = 398$) underwent apolipoprotein E genotyping, MRI, flortaucipir, and ¹¹C-PiB; all 166 Alzheimer's participants were beta-amyloid positive and all controls were beta-amyloid negative. Grey matter volume and flortaucipir standard uptake value ratios were calculated for hippocampus, entorhinal cortex, and neocortex. Ratios of hippocampal-to-neocortical and entorhinal-to-neocortical volume and flortaucipir uptake were also calculated. Linear regression models assessed relationships among regional volume, flortaucipir uptake, and ratios and phenotypes, within three genarians (50–59, 60–69, and 70+). Voxel-level analyses were also performed. **Results:** For 50–59 greater medial temporal atrophy and flortaucipir uptake was observed in the typical compared with atypical phenotype. The typical phenotype also showed greater frontal neocortex uptake with the voxel-level analysis. For 60–69 and 70+ there was greater hippocampal volume loss in the typical compared with atypical phenotype while only the 60–69, but not the 70+ group, showed a difference in hippocampal flortaucipir uptake. We also observed a pattern for higher neocortical flortaucipir uptake to correlate with younger age decade for both phenotypes. **Interpretation:** MRI volumetry versus flortaucipir PET relationships differ across Alzheimer's clinical phenotypes, and also within phenotype across age decades. This suggests that there is potential risk of masked effects by not accounting for genarian in participants with beta-amyloid and tau-positive biomarker defined Alzheimer's disease.

Introduction

Alzheimer's disease is a pathological entity characterized by the presence of beta-amyloid and tau immunoreactive plaques and neurofibrillary tangles.^{1,2} It is well recognized that Alzheimer's disease can have different presenting dementia phenotypes dominated by episodic memory loss, aphasia,

executive dysfunction, ideomotor apraxia, behavioral dyscontrol, dyscalculia, dyslexia, and visuospatial/perceptual deficits.^{3–7} In 2014, the International Working Group (IWG-2) for new Research Criteria for the diagnosis of Alzheimer's disease proposed that all these different presenting phenotypes be collapsed into a simplified classification scheme of two categories: those in which the clinical

phenotype is dominated by episodic memory loss, termed typical Alzheimer's dementia (Ty-AD), and the rest in which nonmemory cognitive signs and symptoms are the dominant characteristic of the syndrome, termed atypical Alzheimer's dementia (Aty-AD).⁸ The IWG-2 also recommended that any diagnosis of Ty-AD and Aty-AD, however, must also be supported by pathophysiological biomarker evidence of underlying beta-amyloid and tau deposition.⁸ This simplified construct of typical and atypical AD as initially envisioned is logical, as it corresponds to a functional/anatomical pattern of brain damage with different relative involvement of medial temporal lobe structures versus neocortical regions.⁹ That is, those with Ty-AD and prominent episodic memory loss show greater damage to allocortical (e.g., hippocampus) and mesocortical (e.g., entorhinal cortex (ERC)) structures compared with neocortex while those with Aty-AD and prominent nonmemory impairment show greater damage to neocortical structures compared with allocortical and mesocortical structures.⁹ Further supporting this classification are the many differences that have been identified between Typical and atypical AD.^{9–13}

Using this well-accepted construct of typical and atypical Alzheimer's dementia, we previously investigated the association between the relative burdens of tau in mesocortex (entorhinal cortex) to neocortex in Ty-AD versus Aty-AD¹⁴ with a PET ligand [¹⁸F] flortaucipir that has been shown to bind to AD type tau.^{15–17} We found that Aty-AD (median age at scan 64) was associated with high neocortical [¹⁸F]flortaucipir uptake but low entorhinal uptake. We found that the Ty-AD phenotype was associated with two different patterns of [¹⁸F]flortaucipir uptake associated with age: one with low uptake in both entorhinal cortex and neocortex in older participants (median age at scan 76), and another with high uptake in both regions associated with younger participants (median age at scan 62). It remains unclear why Ty-AD sexagenarians (individuals age 60–69) would show a different pattern of uptake compared with Ty-AD septuagenarians (age 70+). One possible explanation is that other factors, such as volume loss and/or age, are also crucial to the understanding of Alzheimer's disease phenotypes. Understanding how different biological factors are involved in the different Alzheimer's phenotypes is important for lumping versus splitting phenotypes with regards to regional tissue cellular analyses, genetic association studies, and selecting neuroimaging outcome measures in clinical trials, to name a few.

In this study, we determine whether the relationship between MRI volume and flortaucipir uptake is associated with Alzheimer's phenotype and whether relationships also differ by genarian. We hypothesize that the relationship between hippocampal volume and flortaucipir uptake would differ between Ty-AD and Aty-AD for

older genarians but not for those between 50 and 59, and that relationships would also differ within phenotype across genarians.

Methods

Participants

To be included in this study all participants had to meet published criteria for typical or atypical AD, completed a flortaucipir and Pittsburgh Compound B (PiB) PET scan, and be beta-amyloid positive with a PiB global standardized uptake value ratio (SUVR) of >1.48.¹⁸ We identified 170 participants. After QC of the brain scans, one participant was removed as the MRI scan revealed a large vascular malformation. Three additional subjects were excluded as they were scanned on a Siemens scanner leaving 166 subjects included in this study. These 166 participants from the Mayo Clinic Department of Neurology (86 meeting clinical criteria for Ty-AD and 80 meeting clinical criteria for Aty-AD) were recruited into one of two NIH funded studies between April 7th 2015 and August 1st 2019. The Ty-AD participants were recruited into the Mayo Clinic Alzheimer's Disease Research Center (PI Petersen) while the Aty-AD participants were recruited by the Neurodegenerative Research Group (PI's Josephs and Whitwell). All 86 Ty-AD participants presented with significant and early loss of episodic memory and met DSM IV criteria for AD.¹⁹ All 80 Aty-AD participants presented with predominant visuospatial or visuospatial dysfunction consistent with a diagnosis of posterior cortical atrophy (PCA)²⁰ ($n = 46$) or with a predominant progressive hesitant aphasia with anomia without loss of word meaning and poor sentence repetition consistent with logopenic progressive aphasia (LPA)²¹ also referred to as logopenic variant of primary progressive aphasia²² ($n = 34$). All Ty-AD participants would also meet IWG-2 criteria for typical AD⁸ and all Aty-AD participants would also have met IWG-2 criteria for atypical AD.⁸ All participants underwent a structural MRI brain scan on a General Electric Medical Systems scanner with a 3.0 tesla magnet, a flortaucipir tau-PET scan, and a PiB PET scan, all within a 48-hr window period.

Apolipoprotein E genotype was established with TaqMan chemistry (Applied Biosystems, Carlsbad, CA).

The study was approved by the Mayo Clinic IRB, and all participants consented to participate in this provided written informed consent to participate in this study.

Image acquisition

PET scans were acquired using a PET/CT scanner (GE Healthcare, Milwaukee, Wisconsin) operating in 3D

mode. For tau PET an intravenous bolus injection of approximately 370MBq (range 333–407 MBq) of flortaucipir was administered, followed by a 20-min PET acquisition performed 80 min after injection. The flortaucipir scans consisted of four 5-min dynamic frames following a low-dose CT transmission scan. Standard corrections were applied. Emission data were reconstructed into a 256×256 matrix with a 30-cm field of view (in-plane pixel size = 1.0 mm, slice thickness = 1.96 mm). For PiB-PET an injection of ~ 627 MBq (range 384–722 MBq) of PIB was administered, followed by a 40-min uptake period and a 20-min PIB scan of four 5-min dynamic frames. All participants also underwent a 3T head MRI protocol that included a magnetization prepared rapid gradient echo (MPRAGE) sequence (TR/TE/TI, 2300/3/900 msec; flip angle 8° , 26-cm field of view (FOV); 256×256 in-plane matrix with a phase FOV of 0.94, and slice thickness of 1.2 mm). The MRI scans were performed a median of one day from the flortaucipir and PiB PET scans.

Image processing

Each PET image was rigidly registered to its corresponding MPRAGE using SPM12 (Wellcome Trust Centre for Neuroimaging, London, UK). Using ANTs, the Mayo Clinic Adult Lifespan Template (MCALT) (<https://www.nitrc.org/projects/mcalt/>) atlases were propagated to the native MPRAGE space and used to calculate regional PET values in the grey and white matter. Tissue probabilities were determined for each MPRAGE using Unified Segmentation in SPM12, with MCALT tissue priors and settings. For tau PET, SUVRs were created normalizing uptake in each of three regions of interest (see below) to the cerebellar crus grey matter.²³ For PiB-PET we defined a global PIB SUVR as previously described.²⁴ The MPRAGE space MCALT atlas was also used to calculate regional grey matter volumes. Total intracranial volume was also calculated in order to correct the volume data for head size.

Image analyses

The regions we assessed included an allocortical region (hippocampus = HP), a mesocortical region (entorhinal cortex = ERC), and a neocortical region (neocortex). The neocortical ROI was created by combining the following regions from the MCALT atlas: superior, mid, and inferior occipital cortex + lingual cortex + cuneus + calcarine + angular + superior medial and superior lateral frontal cortex + supramarginal cortex + precuneus + superior and inferior parietal cortex + superior, mid, and inferior temporal cortex. We also assessed neocortex

excluding superior, mid, and inferior temporal cortices given that the lateral temporal lobe is a “hot spot” for flortaucipir uptake and hence could drive the neocortical results. For grey matter volumes, left and right volumes were summed and we calculated volumes adjusted for total intracranial volume using 398 young cognitively normal PiB-negative controls (global PiB SUVR ≤ 1.48), age range between 30 and 50 years old. The cognitively unimpaired controls had been recruited into the Mayo Clinic Study of Aging (MCSA) and underwent the same imaging modalities as the 166 participants. For flortaucipir PET, SUVRs were calculated as a weighted average of left and right median values, scaled by median grey matter cerebellar crus uptake.²³ All analyses were performed without partial volume correction of flortaucipir data in order to keep the grey matter and flortaucipir measurements relatively independent.

Statistical analyses

All 166 Ty-AD and Aty-AD cases were separated by age at scan into three genarians: quinquagenarian (age 50–59), sexagenarian (age 60–69), and septuagenarian (age 70+). These three genarians were selected based on the results of our previous study discussed above,¹⁴ as well as to maintain statistical power. Specifically, we did not have any participants under age 50 and we had only a few participants over age 80. For each of the three ROIs, we fitted a linear regression model with two responses (volume and tau SUVR) with diagnosis (Ty-AD/Aty-AD) and genarian (50–59, 60–69 and 70+) as predictors, and gender included as a nuisance variable. Models also included interactions between diagnosis and genarian to help evaluate whether differences by diagnosis vary by genarian group. Two additional bivariate-response regression models were fitted using ratios. The first model had HP/neocortical volume ratio and HP/neocortical tau ratio. The second had ERC/neocortical volume and ERC/neocortical tau ratio. For each model, within each genarian we performed a linear hypothesis test comparing diagnosis. We used Hypothesis-Error (HE) plots an R package for visualizing hypothesis tests in multivariate linear models to graphically evaluate the results of these hypothesis tests.²⁵ Hypothesis-Error (HE) plots represent sums-of-squares-and-products matrices for linear hypotheses and for error using ellipses (in two dimensions), ellipsoids (in three dimensions), or by line segments in one dimension. The HE plots show a bivariate ± 1 SD error ellipse and a superimposed line corresponding to the contrast. If the line extends outside of the error ellipse the test is significant at $P < 0.05$, indicating group-wise differences. The direction of the line can be used as an indication of how the groups differ (i.e., volume vs. tau vs. both).

In order to determine how well our neuroimaging measures differentiate Ty-AD and Aty-AD within each genarian, we calculated area under the receiver operator characteristic curve (AUROC) values for each neuroimaging measure.

As a secondary analysis, we also split the 80 Aty-AD cases in those with PCA ($n = 46$) versus LPA ($n = 34$) by genarian, for the sole purpose of assessing whether it was reasonable to combine them for this study.

Voxel-level analyses

Voxel-level analyses were performed using SPM12 in order to assess regional patterns of cortical volume loss on MRI and cortical flortaucipir uptake. All MPRAGE scans were spatially normalized to the MCALC template, segmented using unified segmentation, and the grey matter images were modulated and smoothed at 8-mm full-width-at-half-maximum (FWHM). All voxels in the MPRAGE-space flortaucipir images were divided by median uptake in cerebellar crus grey matter to create SUVR images. The images were normalized to the MCALC template using normalization parameters from the MPRAGE normalization and smoothed at 6-mm FWHM.

Comparisons were performed between Ty-AD and Aty-AD, and PiB negative cognitively unimpaired controls from the MCSA that had been matched by age within each genarian. Hence, the 50–59 Ty-AD and Aty-AD groups were matched to 110 controls with a median age at scan of 56 (range 50–59); the 60–69 Ty-AD and Aty-AD groups were matched to 136 controls with a median age at scan of 66 years (range 60–69); and the 70+ Ty-AD and Aty-AD groups were matched to 152 controls with a median age at scan of 77 years (range 70–94). All voxel-level analyses were performed using multiple regression models in SPM12 and results were assessed corrected for multiple comparisons using the family-wise error (FWE) correction at $P < 0.05$.

Results

There were demographic and clinical differences between Ty-AD and Aty-AD as shown in Table 1. When stratified by genarian, the 70+ Ty-AD participants were on average 4 years older (78 vs. 74 years old), and the disease duration was 2 years longer (3.0 vs. 5.1 years), than the 70+ Aty-AD participants. The PiB SUVR also differed by phenotype in the 70+ genarian, where the Ty-AD participants had higher PiB SUVR than Aty-AD (2.66 vs. 2.27). In fact, the 70+ Aty-AD participants did not follow the expected trend of increasing PiB SUVR with increasing age by decade. For clinical measures, as expected the Ty-

AD participants performed worse on the MoCA and on the AVLT test of recall compared with Aty-AD across all genarians while the Aty-AD participants performed poorer on the Rey-Osterrieth Complex Figure compared with the Ty-AD participants.

Overall linear regression results

There were differences in how volume and tau were related to each other between typical and atypical groups and across genarians, for all the neuroimaging outcomes ($P \leq 0.001$).

Phenotype differences by genarian

We found evidence for different relations between Ty-AD and Aty-AD in all three genarians.

In the 50–59 genarian (Fig. 1), there was some indication that for hippocampus the Ty-AD participants had more flortaucipir uptake and greater volume loss. The two groups had similar levels of neocortical uptake and volume loss. The analyses of the ratios suggest if anything differences were in terms of volumes. We note, however, that the signal is not strong in this younger age group.

In the 60–69 genarian (Fig. 2), the overall pattern was generally similar but was more striking. The Ty-AD cases had more severe hippocampal involvement in terms of both uptake and volume. A comparatively large difference was found in terms of neocortical involvement limited primarily to the volume dimension with Aty-AD cases having greater volume loss. For the ratio analyses, the group-wise differences were highly significant due to both flortaucipir uptake ratio and volume ratio differences and emphasize that the Ty-AD individuals have comparatively more hippocampal and ERC involvement for a given neocortical involvement.

In the 70+ genarian (Fig. 3), there were similarities, as well as differences, observed, from the 60–69 genarian. For hippocampus, Ty-AD cases were more severe in terms of volume loss but unlike in the 60–69 genarian there was little difference in flortaucipir uptake. For ERC, both volume and flortaucipir uptake differences were observed. In neocortex, we observed a difference between Aty-AD and Ty-AD that was mainly driven by flortaucipir uptake. The two ratio measures were similar to those observed for the 60–69 genarian, and again highly significant, indicating more hippocampal and ERC severity for typical AD cases relative to neocortical involvement.

When we assessed the results using neocortex minus lateral temporal cortices instead of “the whole neocortex” the results were identical to those of the whole neocortex, suggesting that the neocortical results were not driven by lateral temporal neocortex (Fig. S1).

Table 1. Demographic and clinical characteristics of all participants.

	CU (n = 398)	Atypical AD (n = 80)	Typical AD (n = 86)	P-value between ADs	PCA (n = 46)	LPA (n = 34)	P-value PCA vs. LPA
Female	180 (45%)	55 (69%)	45 (52%)	0.04	33 (72%)	22 (65%)	0.63
Age at MRI, y							
All	67 (50, 95)	65 (53, 80)	71 (52, 90)	0.005	63 (55, 77)	68 (53, 80)	0.10
Age 50–59	56 (50, 59.9)	57 (53, 59.9)	55 (52, 60)	0.03	57 (55, 60)	57 (53, 59)	0.97
Age 60–69	66 (60, 69.8)	65 (60, 69.7)	64 (60, 69)	0.70	64 (60, 70)	66 (61, 69)	0.21
Age 70 and over	77 (70, 95.0)	74 (70, 80.0)	78 (70, 90)	0.002	73 (70, 77)	75 (70, 80)	0.25
Age levels				0.03			0.39
50–59	110 (28%)	21 (26%)	15 (17%)		13 (28%)	8 (24%)	
60–69	136 (34%)	33 (41%)	26 (30%)		21 (46%)	12 (35%)	
70 and over	152 (38%)	26 (32%)	45 (52%)		12 (26%)	14 (41%)	
Education, y	16 (9, 20)	16 (12, 25)	14 (8, 20)	0.01	16 (12, 25)	16 (12, 20)	0.96
Age at onset, y	NA	61 (43, 77)	64 (48, 88)	0.15	58 (50, 75)	64 (43, 77)	0.01
Disease duration, y							
All	NA	3.1 (1.0, 18.0)	4.5 (0.6, 17.2)	<0.001	4.0 (1.0, 18.0)	3.0 (1.0, 10.0)	0.01
Age 50–59	NA	3.0 (1.0, 10.0)	4.0 (2.2, 5.9)	0.07	3.0 (1.0, 6.2)	2.0 (1.0, 10.0)	0.28
Age 60–69	NA	4.0 (1.0, 12.0)	4.3 (1.2, 17.2)	0.26	4.0 (1.0, 12.0)	2.8 (1.0, 6.0)	0.03
Age 70 and over	NA	3.0 (1.0, 18.0)	5.1 (0.6, 12.9)	0.02	3.9 (1.0, 18.0)	3.0 (2.0, 9.3)	0.44
APOE carrier							
All	88/388 (23%)	29/61 (48%)	63/82 (77%)	<0.001	15/34 (44%)	14/27 (52%)	0.61
Age 50–59	32/105 (30%)	5/16 (31%)	9/15 (60%)	0.16	3/10 (30%)	2/6 (33%)	>0.99
Age 60–69	30/134 (22%)	12/24 (50%)	21/24 (88%)	0.01	7/15 (47%)	5/9 (56%)	>0.99
Age 70 and over	26/149 (17%)	12/21 (57%)	33/43 (77%)	0.15	5/9 (56%)	7/12 (58%)	>0.99
PiB SUVRs							
All	1.36 (1.14, 1.48)	2.43 (1.50, 4.66)	2.51 (1.55, 3.38)	0.09	2.44 (1.54, 3.07)	2.38 (1.50, 4.66)	0.97
Age 50–59	1.32 (1.14, 1.46)	2.45 (1.78, 3.20)	2.46 (1.76, 3.02)	0.97	2.48 (2.00, 3.07)	2.76 (1.93, 4.66)	0.70
Age 60–69	1.35 (1.17, 1.48)	2.48 (1.93, 4.66)	2.47 (1.55, 3.02)	0.28	2.48 (2.00, 3.07)	2.76 (1.93, 4.66)	0.20
Age 70 and over	1.38 (1.20, 1.48)	2.27 (1.50, 3.02)	2.66 (1.60, 3.38)	0.002	2.35 (1.54, 2.83)	2.21 (1.50, 3.02)	0.78
MoCA							
All		18 (0, 26)	14 (0, 25)	<0.001	16 (1, 26)	19 (0, 26)	0.46
Age 50–59		17 (2, 25)	8 (0, 21)	0.04	17 (2, 25)	16 (6, 25)	0.80
Age 60–69		17 (1, 25)	14 (1, 25)	0.13	16 (1, 25)	20 (12, 25)	0.18
Age 70 and over		18 (0, 26)	14 (1, 23)	0.01	18 (10, 26)	18 (0, 26)	0.79
AVLT delayed % recall MOANS*							
All		6.0 (2.0, 17.0)	5.0 (2.0, 15.0)	0.002	6.0 (2.0, 17.0)	6.0 (2.0, 11.0)	0.63
Age 50–59		6.5 (2.0, 11.0)	2.0 (2.0, 7.0)	0.08	7.0 (2.0, 11.0)	5.0 (2.0, 9.0)	0.49
Age 60–69		6.0 (2.0, 11.0)	4.0 (2.0, 7.0)	0.04	5.0 (2.0, 10.0)	6.0 (2.0, 11.0)	0.47
Age 70 and over		6.5 (3.0, 17.0)	5.0 (3.0, 15.0)	0.04	8.0 (4.0, 17.0)	6.0 (3.0, 11.0)	0.27
Rey-Osterrieth figure							
All		2.0 (2.0, 13.0)	7.0 (2.0, 14.0)	<0.001	2.0 (2.0, 9.0)	5.5 (2.0, 13.0)	<0.001
Age 50–59		2.0 (2.0, 11.0)	8.0 (5.0, 12.0)	0.003	2.0 (2.0, 2.0)	3.5 (2.0, 11.0)	0.02
Age 60–69		2.0 (2.0, 12.0)	5.0 (2.0, 11.0)	0.13	2.0 (2.0, 2.0)	6.0 (2.0, 12.0)	<0.001
Age 70 and over		2.0 (2.0, 13.0)	7.0 (2.0, 14.0)	0.06	2.0 (2.0, 9.0)	6.0 (2.0, 13.0)	0.08

Data shown are n (%) or median (range). For categorical variables, *P*-values are from Fisher's Exact tests. For continuous variables, *P*-values are from Wilcoxon Rank Sum tests.

AD, Alzheimer's dementia; APOE ε4, apolipoprotein epsilon 4; AVLT, auditory verbal learning test; CU, cognitively unimpaired; MoCA, Montreal Cognitive Assessment; PCA, posterior cortical atrophy; LPA, logopenic progressive aphasia.

*Data shown as Mayo Older American Normative (MOANS) scores with average = 10 and Standard deviation = 3.

Differences within clinical phenotype by genarian

Interaction tests of whether group-wise differences varied with genarian provided some evidence of age-specific differences in relationship, within phenotype ($P = 0.05$).

Among the Ty-AD group, both hippocampus and ERC followed a pattern whereby the youngest group had the most tau but the least atrophy and the oldest group had the least tau yet the most atrophy (Fig. 4). For both the Ty-AD and Aty-AD participants, neocortical uptake was highest in the 50–59 genarian and decreased to the oldest

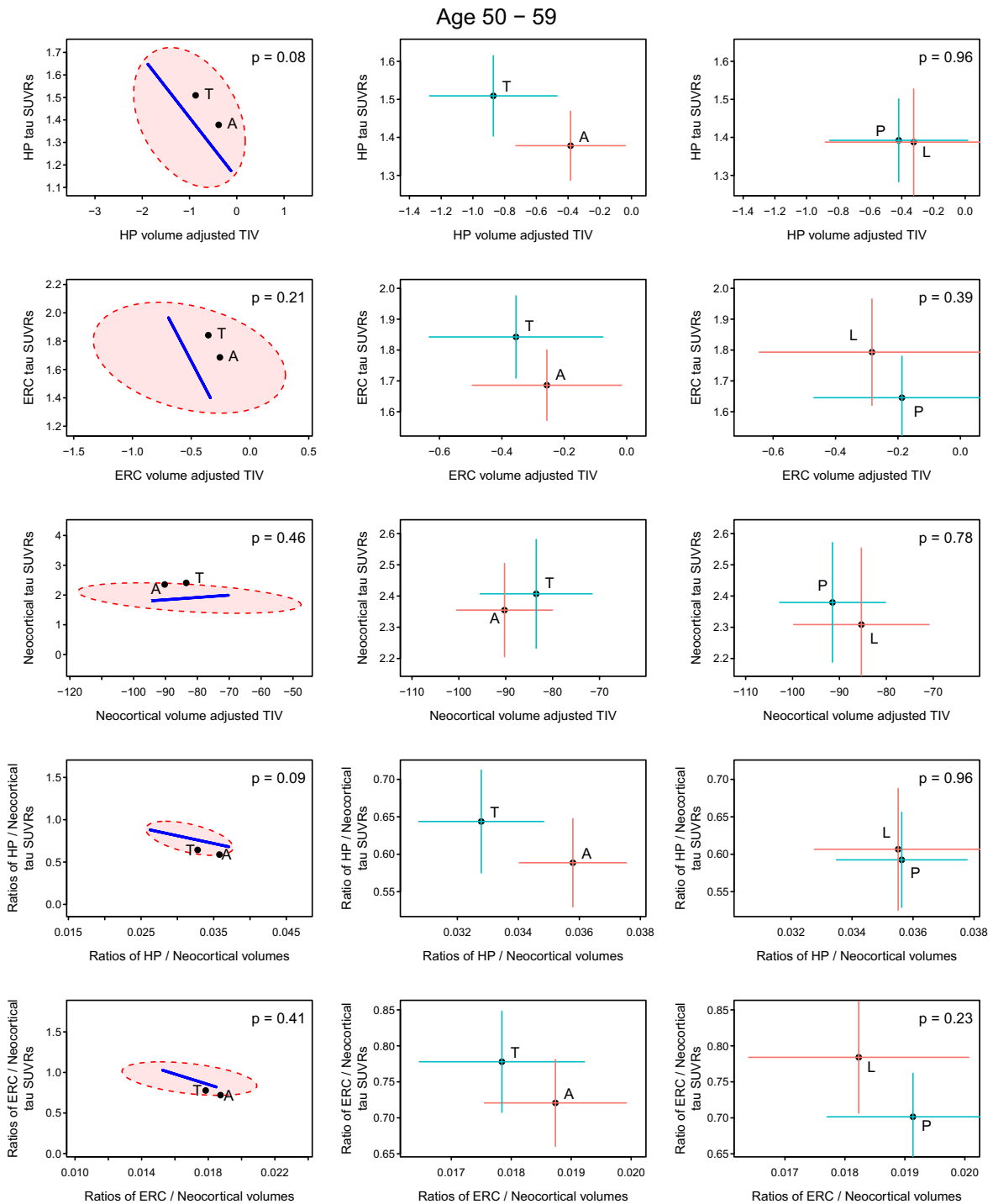


Figure 1. Volume and flortaucipir uptake within the 50–59 geriatrician. Significance scaling hypothesis error plots are shown in the left column. The ellipse represents within-group variation (how much the individuals vary from the group mean), with the line representing between-group (i.e., Ty-AD (T) vs. Aty-AD (A)) variation. Significance scaling was applied so that if the line extends outside the ellipse, the multivariate test is significant at $P < 0.05$ (P values shown in each plot). The black dots represent group means for atypical and typical phenotypes. The plots in the middle (atypical AD vs. typical AD) and right (PCA (P) vs. LPA (L)) columns show estimated group means with 95% confidence interval error bars (red vertical for flortaucipir and blue horizontal for volume). If error bars do not cross then group means can be considered significantly different. The greater the separation of the crosses the more significant the difference, which applies to vertical and horizontal separations for the variables labeled on each axis.

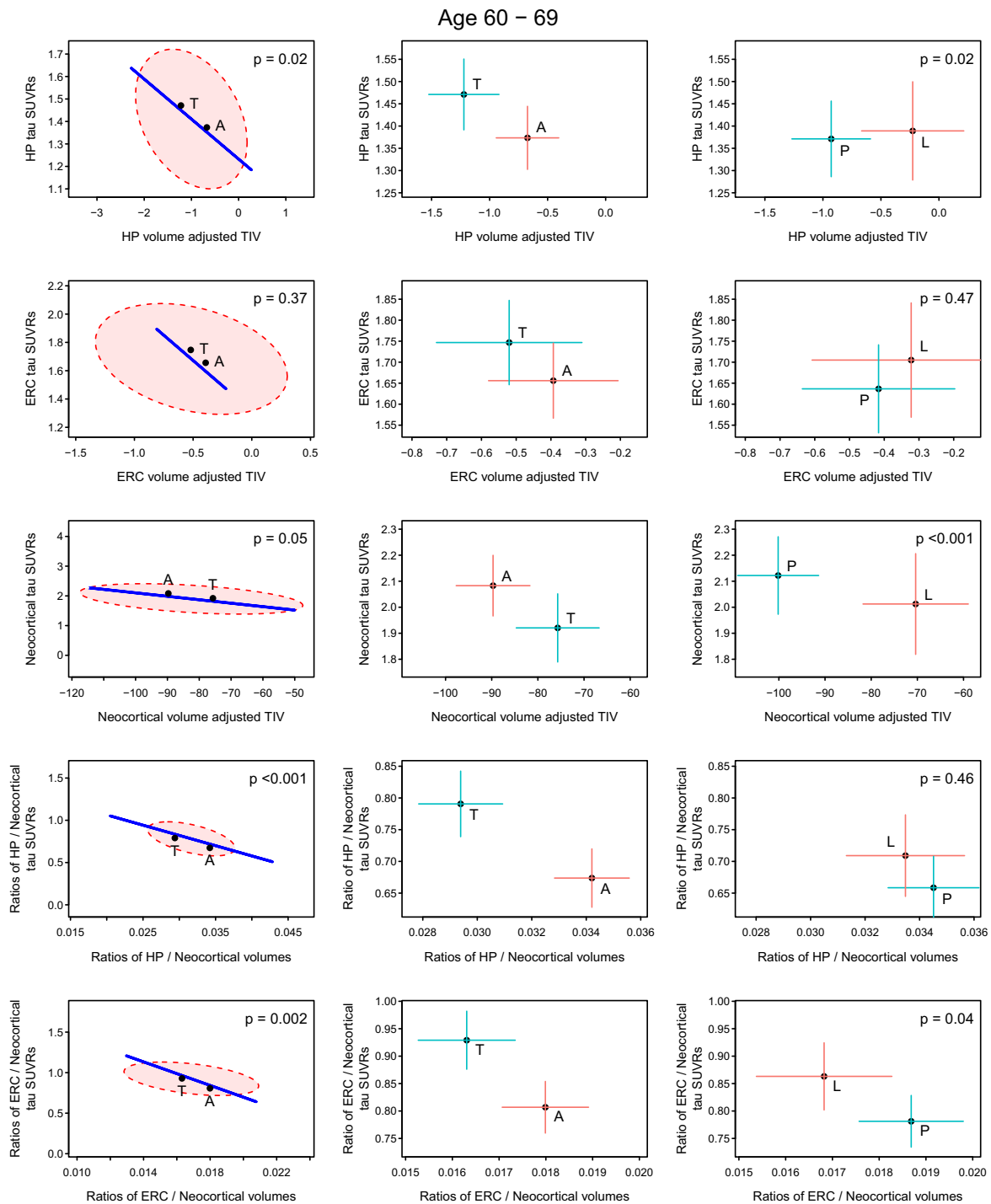


Figure 2. Volume and flortaucipir uptake within the 60–69 geriatrician. Significance scaling hypothesis error plots are shown in the left column. The ellipse represents within-group variation (how much the individuals vary from the group mean), with the line representing between group (i.e., Ty-AD (T) vs. Aty-AD (A)) variation. Significance scaling was applied so that if the line extends outside the ellipse the multivariate test is significant at $P < 0.05$ (P values shown in each plot). The black dots represent group means. The plots in the middle (atypical AD vs. typical AD) and right (PCA (P) vs. LPA (L)) columns show estimated group means with 95% confidence interval error bars (red vertical for flortaucipir uptake and blue horizontal for volume). If error bars do not cross then group means can be considered significantly different. The greater the separation of the crosses the more significant the difference, which applies to vertical and horizontal separations for the variables labeled on each axis.

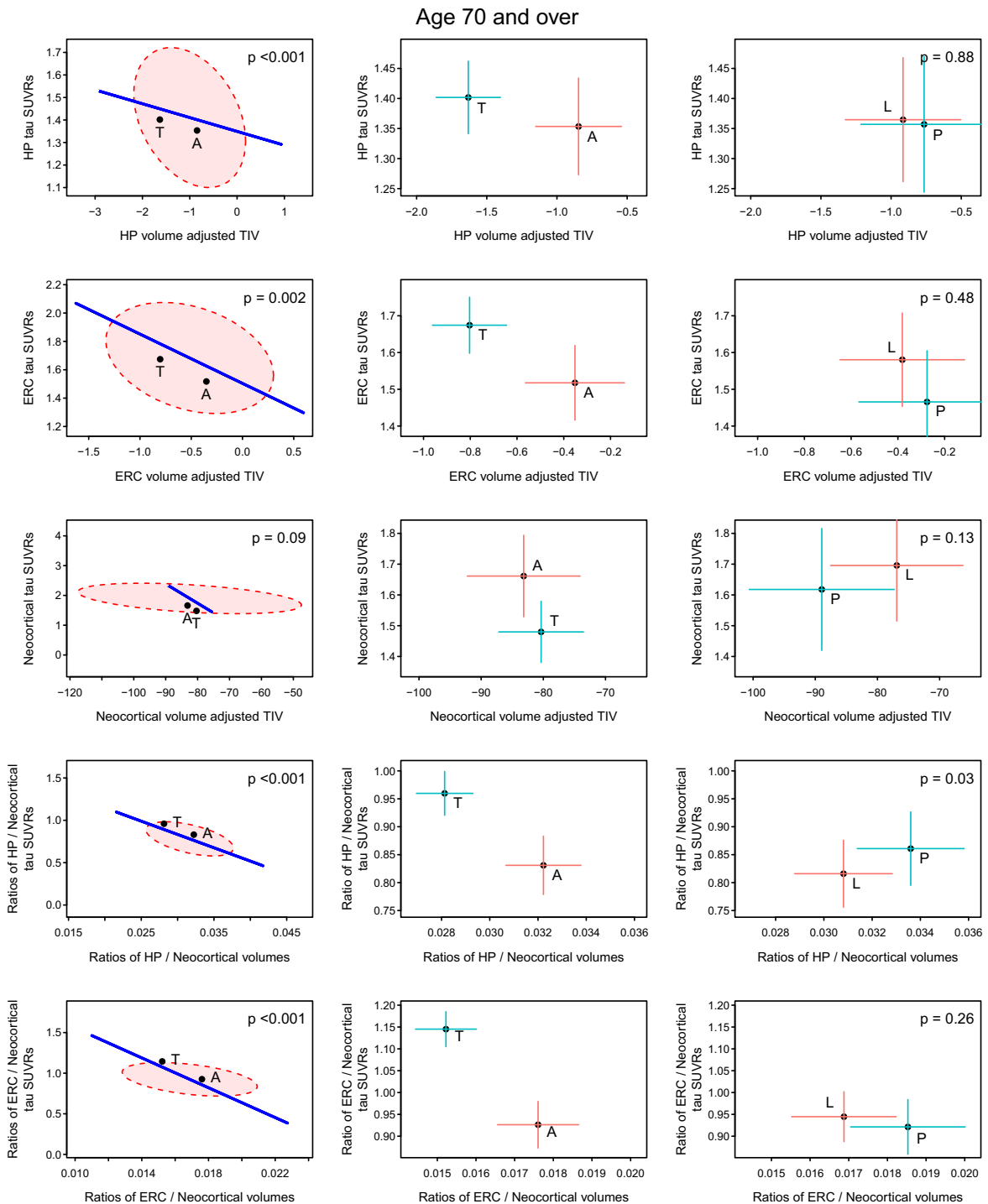


Figure 3. Volume and flortaucipir findings across AD phenotypes within the 70+ generation. Significance scaling hypothesis error plots are shown in the left column. The ellipse represents within-group variation (how much the individuals vary from the group mean), with the line representing between-group (i.e., Ty-AD (T) vs. Aty-AD (A)) variation. Significance scaling was applied so that if the line extends outside the ellipse the multivariate test is significant at $P < 0.05$ (P values shown in each plot). The black dots represent group means. The plots in the middle (atypical AD vs. typical AD) and right (PCA (P) vs. LPA (L)) columns show estimated group means with 95% confidence interval error bars (red vertical for flortaucipir and blue horizontal for volume). If error bars do not cross then group means can be considered significantly different. The greater the separation of the crosses the more significant the difference which applies to vertical and horizontal separations for the variables labeled on each axis.

genarian without any observable differences in volume. For both ratio measures, in Ty-AD there was a gradient such that the 70+ genarian had the most relative medial temporal involvement for both tau ratio and volume ratio and the 50–59 genarian had the least. For both ratios, the differences were clearest in the tau dimension. For the ratios, the Aty-AD group had an overall pattern that was similar to that of the Ty-AD group with the oldest age group having the largest uptake ratios and the smallest volume ratios and the youngest age group showing the opposite relationship. The separation between the Aty-AD genarian groups was less, however, compared with the typical genarian groups.

AUROC results

None of the AUROC estimates provided good differentiation of Ty-AD from Aty-AD in the 50–59 genarian (Table S1). For the 60–69 and 70+ genarians, there was evidence for some outcome measures being able to provide good differentiation of Ty-AD from Aty-AD. The HP/Cortex volume ratio, although not always the highest estimate for the genarian, appears to be a useful measure to differentiate Aty-AD from Ty-AD (lower ratio suggest Ty-AD). For 70+ participants the ERC/Cortical flortaucipir uptake ratio provided the highest estimate to differentiate Ty-AD from Aty-AD (higher uptake ratio suggests Ty-AD).

Posterior cortical atrophy compared with logopenic progressive aphasia

Not many differences were observed in demographic or clinical features between PCA and LPA (Table 1). The PCA participants had longer disease duration in the 60–69 genarian (4.0 vs. 2.8 years). As expected, PCA participants performed more poorly on the Rey-O Complex Figure Test. For the neuroimaging outcome measures, in the majority of instances, there was little evidence that PCA differed from LPA, across the three genarians (Figs. 1–3). The one exception was that PCA patients had smaller neocortical volumes than LPA patients especially for the 60–69 genarian.

Voxel-level analysis findings

For volume, Aty-AD showed greater left medial and lateral occipital loss compared with Ty-AD in the 60–69 age decade, and Ty-AD showed greater hippocampal volume loss compared with Aty-AD in the 70+ age decade (Figs. 5 and 6). No other group differences were identified in volume. However, there were differences in cortical flortaucipir uptake in all three genarians (Figs. 5 and

6). For 50–59, Ty-AD showed greater flortaucipir uptake in bilateral prefrontal cortex compared with Aty-AD, while Aty-AD showed greater uptake in left occipital cortex compared with Ty-AD. For 60–69, Aty-AD showed greater uptake in left occipital and sensorimotor cortex compared with Ty-AD, while Ty-AD showed greater hippocampal uptake compared with Aty-AD. For 70+, Aty-AD showed greater uptake in left occipital, posterior superior temporal, supramarginal, and superior parietal cortices compared with Ty-AD while Ty-AD showed more hippocampal uptake compared with Aty-AD.

Interpretation

In this study, we attempted to try to better understand how volume and flortaucipir uptake are related to AD phenotypes and genarian (age by decade). We found that relationships between hippocampal, ERC, and neocortical volume loss and flortaucipir uptake differed between the two AD clinical phenotypes within age decade, and that some relationships also differed within phenotype, across age decades.

The Ty-AD participants in the 50–59 genarian were unusual. This group did not show the neuroimaging signatures we saw in the 60–69 and 70+ Ty-AD groups. There was indeed evidence for greater hippocampal atrophy and flortaucipir uptake compared with the Aty-AD group which supports the typical diagnosis but medial temporal involvement was not striking, as we observed in the 60–69 and 70+ genarians. In addition, in our voxel-level neuroimaging analysis, we found only the 50–59 Ty-AD participants to have greater flortaucipir uptake in the frontal neocortex compared with Aty-AD. Unlike the Ty-AD participants, the Aty-AD participants in this genarian showed more similar neuroimaging relationships compared with the Aty-AD participants in the 60–69 age decade.

In the 60–69 genarian, we found clinical and neuroimaging characteristics expected of both phenotypes. We found greater hippocampal involvement in both volume and flortaucipir uptake in Ty-AD compared with Aty-AD. Conversely, the Aty-AD participants showed greater neocortical atrophy and more flortaucipir uptake in posterior neocortical regions of the brain compared with Ty-AD. We also found striking differences in the HP/cortical and ERC/cortical ratios for both volume and uptake, with these ratios showing the highest AUROC values for differentiating the phenotypes.

For the 70+ genarian, we observed a difference in hippocampal volumes with smaller volumes occurring in Ty-AD compared with Aty-AD as we did for the 60–69 genarian. In fact, the hippocampal volumes were smallest in the Ty-AD participants in this genarian. Intriguingly, however, in contrast to the 60–69 genarian, we did not

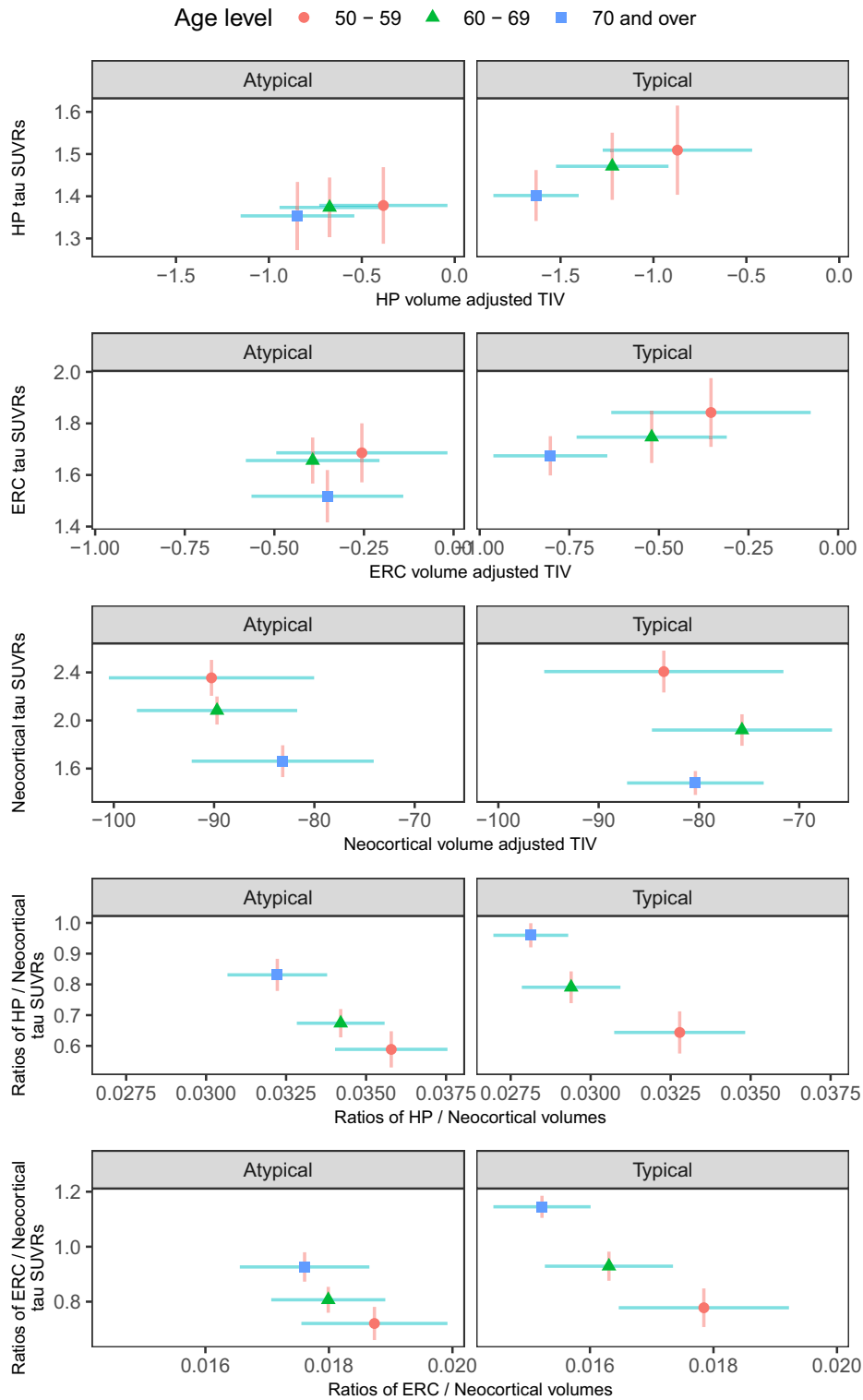


Figure 4. Volume and flortaucipir findings across genearians for Aty-AD and Ty-AD. Plots show estimated group means for each genearian with 95% confidence interval error bars (red vertical for flortaucipir and blue horizontal for volume). If error bars do not cross then group means can be considered significantly different. The greater the separation of the crosses the more significant the difference which applies to the vertical and horizontal separations for the variables labeled on each axis.

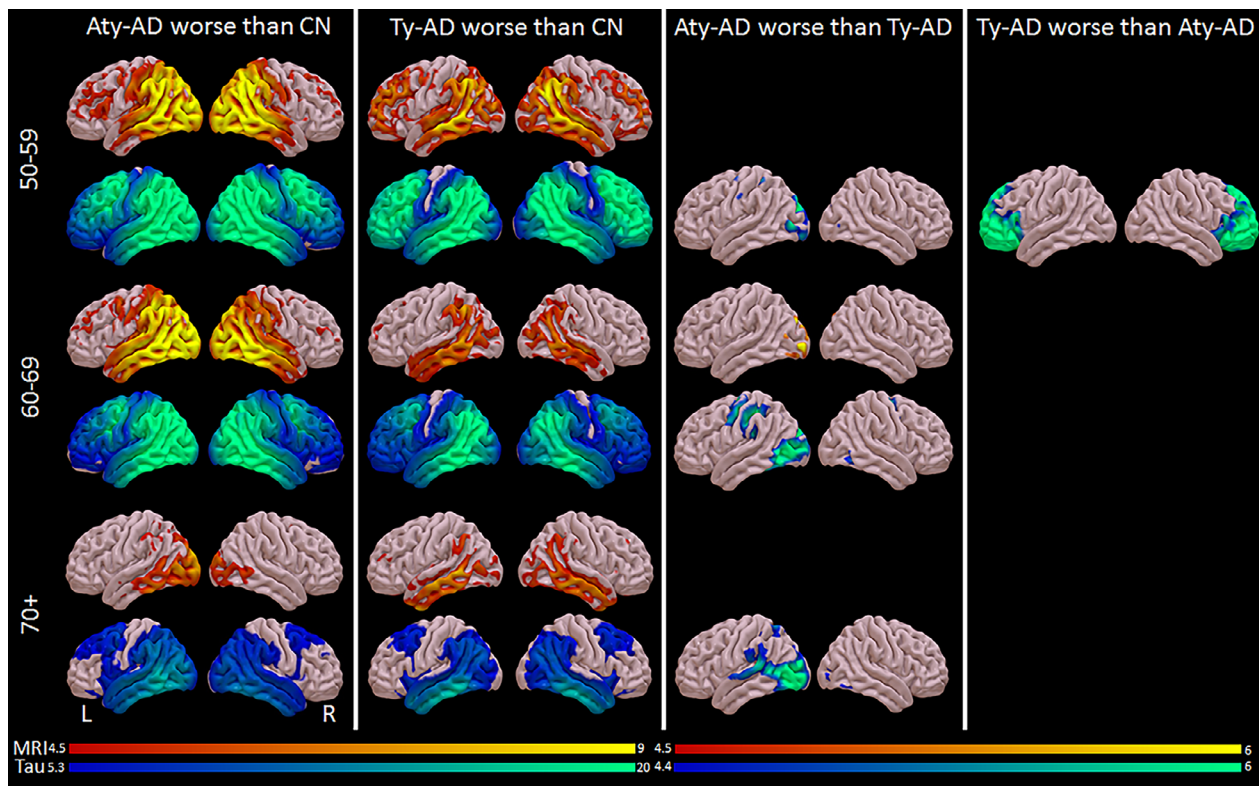


Figure 5. Voxel-level cortical volume (red/yellow) and flortaucipir (blue/green) findings across phenotypes and genarians. Results are shown on three-dimensional brain renderings created using the Surf ice software program (www.nitrc.org). Grey matter volume results are shown corrected for multiple comparisons using FWE at $P < 0.05$. Flortaucipir results comparing AD groups with controls (first two columns) are shown corrected for multiple comparisons using FWE correction at $P < 0.0001$ because results were so extensive, and comparing the two AD groups (third column) are shown corrected for multiple comparisons using FWE at $P < 0.05$.

observe a difference in hippocampal flortaucipir uptake between the phenotypes. This would suggest that for the 70+ participants there are factors other than tau that are playing a role in the hippocampal volume differences. Similar to the hippocampus, we found greater ERC atrophy in Ty-AD compared with Aty-AD. In addition, in the 70+ genarian only, we also observed a difference in flortaucipir ERC uptake. This is worth some discussion, however, as the explanation for this latter difference is complex. Taking into account what is happening in the 60–69 genarian, it seems that the difference in ERC volume in the 70+ genarian is due to the Ty-AD participants having a large degree of volume loss. The difference in ERC flortaucipir uptake, however, in the 70+ genarian appears to be driven by what is happening with the Aty-AD participants, more so than what is happening with the Ty-AD participants. Specifically, when compared with the 60–69 genarian, the 70+ Aty-AD participants had relatively less uptake in the ERC, as opposed to the Ty-AD participants having relatively more uptake. It therefore appears that the relationship between volume loss and

atrophy in the 70+ genarian for Ty-AD participants is not identical to the relationship in the 60–69 genarian for Ty-AD. And while our study was not designed to identify such factors, we speculate, based on the published literature, that one such factor that could be playing a role in the oldest genarian is another protein known as the TAR DNA binding protein of 43 kDa (TDP-43).²⁶ TDP-43 has been found to be associated with older age and with hippocampal volume loss in AD,^{27,28} although not in Aty-AD.^{11,29} Other factors that may also be playing a role in this age group include hippocampal sclerosis, a pathological process which is related to TDP-43,³⁰ vascular disease, Lewy body disease, and argyrophilic grains disease.^{31–33}

For the 70+ genarian, we also observed the Aty-AD group to be somewhat different from the Aty-AD group in the 60–69 and 50–59 genarians. First, it remains unclear why the Aty-AD participants in the 70+ genarian had relatively less ERC flortaucipir uptake than the Aty-AD groups in the 60–69 and 50–59 genarians. Second, we also found beta-amyloid deposition to be lower in Aty-AD compared with the Ty-AD in the 70+ genarian. In

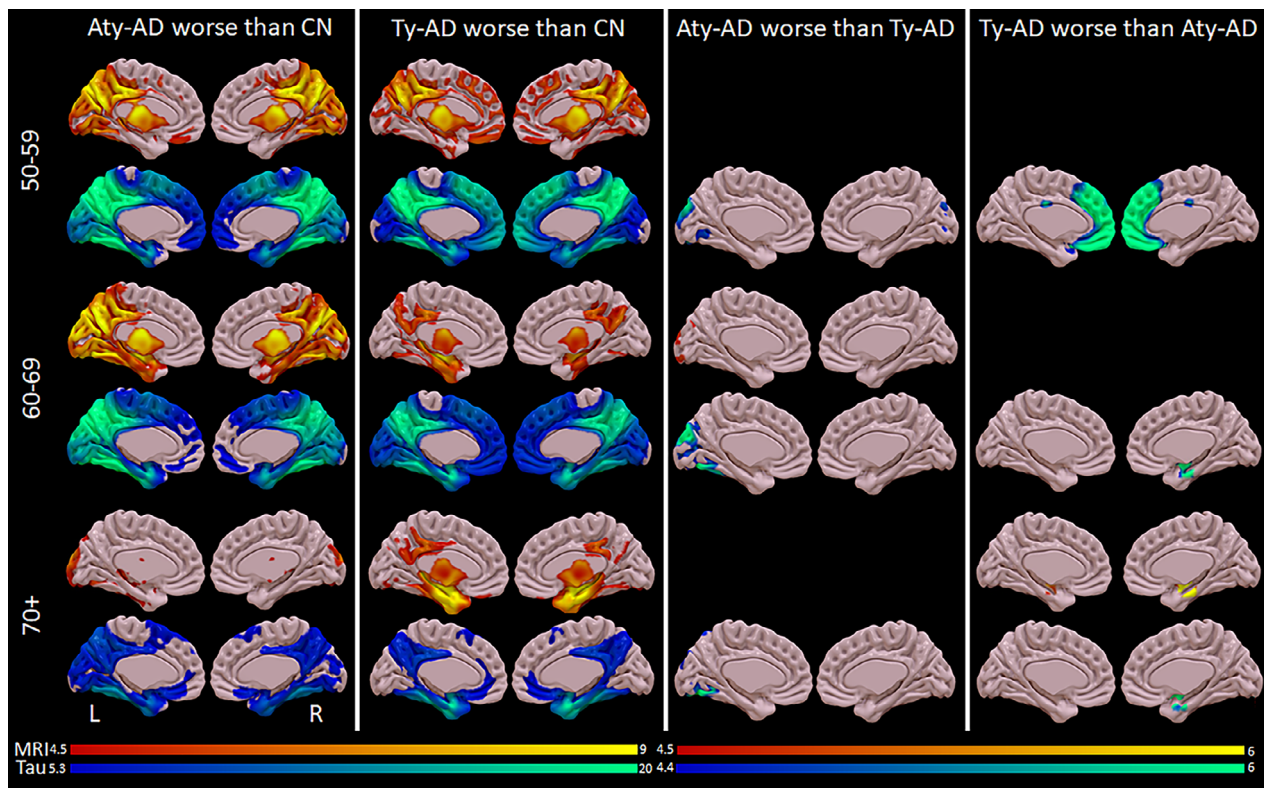


Figure 6. Voxel-level medial volume (red/yellow) and flortaucipir (blue/green) findings across phenotypes and genarians. Results are shown on medial surface brain renderings created using the Surf ice software program (www.nitrc.org). Grey matter volume results are shown corrected for multiple comparisons using FWE at $P < 0.05$. Flortaucipir results comparing AD groups with controls (first two columns) are shown corrected for multiple comparisons using FWE correction at $P < 0.0001$ because results were so extensive, and comparing the two AD groups (third column) are shown corrected for multiple comparisons using FWE at $P < 0.05$.

fact, while in Ty-AD, PiB SUVR increased going from younger to older genarian as expected, the PiB SUVR values increased in Aty-AD from 50–59 to 60–69 but then unexpectedly decreased; in fact it was lowest in Aty-AD in the 70+ genarian. The reason for this phenomenon remains unclear but one explanation could be related to other pathological factors also being at play in the 70+ Aty-AD participants, such as corticobasal degeneration and cerebral amyloid angiopathy, which are pathologies that have been associated with an Aty-AD phenotype in this genarian.^{34–36}

Differentiating between Ty-AD and Aty-AD within genarian may best be accomplished with the use of ratios, although doing so for the 50–59 genarian requires further study. One possible option to differentiate phenotypes in the 50–59 genarian is to use the product of flortaucipir uptake in frontal neocortex and flortaucipir uptake in hippocampus (Frontal-tau X Hippo-tau) with the expectation of higher products for Ty-AD and lower products for Aty-AD. The HP/Cortical volume ratio appears to be useful to differentiate the phenotypes in the 60–69 and 70+

genarians, although for the latter genarian an ERC/cortical ratio may prove better. These results are in keeping with our previous study showing that a HP/cortical volume ratio can be useful at differentiating different subtypes of AD.³⁷

We found a strong association between neocortical flortaucipir uptake and age, with younger participants in both phenotypes showing greater cortical uptake than older participants. This association with age was, however, not observed with neocortical volume. This confirms our previous findings within atypical AD,³⁸ and another study that found greater neocortical flortaucipir uptake in younger age participants.³⁹ It also explains why in one recent pathological study, higher neurofibrillary tangle burden was found in the Aty-AD cases compared with Ty-AD cases where the latter group was older.⁴⁰ This mismatch between flortaucipir uptake and volume in the relationship with age could be due to a number of different factors. It is possible that cortical tau deposition precedes cortical atrophy and hence cortical atrophy has not yet caught up with the degree of cortical flortaucipir

uptake. It is also possible that the sensitivity of neocortical tau and volume detection with PET and MRI, respectively, differ, with the latter being less sensitive. In fact, we have shown that tau uptake on flortaucipir is more closely correlated with FDG-PET hypometabolism than MRI atrophy.⁴¹ Lastly, although we cannot entirely exclude the possibility that cortical tau dissociates from cortical atrophy, we do not have evidence to support this biology. Generally, we did not observe correlations between age and the medial temporal measures, with the exception that Ty-AD participants over the age of 70 showed smaller hippocampal volumes than the 50–59 Ty-AD participants, despite having the lowest degree of flortaucipir uptake. As discussed above, this could be due to the contribution of multiple different pathologies, particularly TDP-43.

Prior voxel-level analyses have found different regional patterns of cortical volume loss^{42–44} and flortaucipir uptake in the cortex^{45–48} between PCA and LPA. The aim of our study was not to identify regional differences between PCA and LPA, and hence we did not repeat these studies. However, using our neuroimaging metrics we found similar relationships between volume loss and flortaucipir uptake when assessing mesial temporal lobe and neocortex as a whole, as opposed to regionally, suggesting that the biology underlying PCA and LPA, and how these syndromes differ from Ty-AD, are in general similar. There were some differences in the 60–69 genarian, with PCA showing worse atrophy, although this was expected given their longer disease duration in this genarian.

This study has several strengths. First, we had a large number of prospectively recruited Ty-AD and Aty-AD participants from two large NIH-funded grants including a large number with LPA and PCA. Secondly, all 567 Alzheimer's disease and healthy controls underwent identical neuroimaging protocols and those with Alzheimer's were well characterized clinically, with the majority completing APOE genotyping. We also performed both ROI-level analyses as well as voxel-level analysis of flortaucipir uptake and volume loss. One potential limitation worth mentioning is that flortaucipir uptake in the hippocampus should be cautiously interpreted as it has been argued to be affected by the spatial resolution of PET, especially in cases of significant hippocampal atrophy,⁴⁹ and from bleed in of signal from adjacent choroid plexus.^{16,50} For these reasons, we also analyzed the ERC as another medial temporal region. We cannot ignore the hippocampal findings, however, as hippocampal flortaucipir uptake correlated with autopsy determined paired helical filament tau burden in one study,¹⁸ supporting flortaucipir hippocampal measurement as valid. Our separation by genarian is not a limitation as it was the aim of the study. While age 65 has been accepted as the "traditional" cut-

point for early-onset versus late-onset Alzheimer's disease, it remains unclear whether this age cut-point is valid. We specifically assessed genarian as age decades are easily interpretable and meaningful to everyone. Had we split the cohort into equal numbers we would have had very odd cut-points that would be meaningless. Furthermore, by analyzing the data by genarian as we did, we do not make any assumptions about directionality (i.e., one genarian has more or less volume loss or flortaucipir uptake than the other), and our analysis allows for some nonlinear age effects in an understandable manner. One pitfall which we avoid and which is worth mentioning explicitly is that the patterns we observe in those in the 70+ age group are not an indication of what those in the youngest age group will look like 15–20 years later. Furthermore, the individuals in the oldest genarian are those who had a relatively favorable disease course: they tended to be "dementia free" for longer. Consequently, inferences from the data should not be about prior or future patterns but rather about patterns we see for a particular category of patient.

In summary, we investigated biological underpinnings of the atypical and typical AD phenotypes across three genarians and found that the phenotypes have heterogeneous biological underpinning, with evidence for heterogeneity across genarian. Therefore, there is the potential risk of masked effects by not accounting for age genarian in participants with beta-amyloid and tau-positive biomarkers, and even more so by not accounting for phenotype.

Acknowledgments

The work was supported by grants from the National Institutes of Health (R01 AG50603 (JLW), P50-AG016574 (RCP), P30 AG062677 (RCP) and U01-AG006786 (RCP)) and The Elsie and Marvin Dekelboum Family Foundation and the Oxley Foundation. We thank AVID Radiopharmaceuticals, Inc., for their support in supplying the AV-1451 precursor, chemistry production advice and oversight, and FDA regulatory cross-filing permission and documentation needed for this work.

Conflicts of Interest

Petersen received personal fees from Roche, Merck, Biogen, Genentech, Eisai, and GE Healthcare outside the submitted work. Lowe serves as a consultant for Bayer Schering Pharma, Philips Molecular Imaging, Piramal Imaging, and GE Healthcare outside the submitted work and receives research support from GE Healthcare, Siemens Molecular Imaging, and AVID Radiopharmaceuticals related to PET imaging.

Authors Contributions

KAJ was responsible for study concept and design, data interpretation, and drafting the original report which was reviewed and revised by JLW, NT, JGR SDW, MB, CGS, MLS, NT, DTJ, MMM, BFB, DSK, VJL, CRJ, and RCP. CRJ, VJL, and JLW were responsible for acquisition of the flortaucipir and volume data. JLW, CGS, and MLS were responsible for all neuroimaging analyses. NT and SDW were responsible for statistical analysis. KAJ, JGR, DTJ, BFB, DSK, and RCP were responsible for acquisition of the clinical data. Funding was obtained by JLW and RCP.

References

- Hyman BT, Phelps CH, Beach TG, et al. National Institute on Aging-Alzheimer's Association guidelines for the neuropathologic assessment of Alzheimer's disease. *Alzheimers Dement* 2012;8:1–13.
- Montine TJ, Phelps CH, Beach TG, et al. National Institute on Aging-Alzheimer's Association guidelines for the neuropathologic assessment of Alzheimer's disease: a practical approach. *Acta Neuropathol* 2012;123:1–11.
- Sakae N, Josephs KA, Litvan I, et al. Clinicopathologic subtype of Alzheimer's disease presenting as corticobasal syndrome. *Alzheimers Dement* 2019;15:1218–1228.
- Snowden JS, Thompson JC, Stopford CL, et al. The clinical diagnosis of early-onset dementias: diagnostic accuracy and clinicopathological relationships. *Brain* 2011;134(Pt 9):2478–2492.
- Renner JA, Burns JM, Hou CE, et al. Progressive posterior cortical dysfunction: a clinicopathologic series. *Neurology* 2004;63:1175–1180.
- Mesulam M, Wicklund A, Johnson N, et al. Alzheimer and frontotemporal pathology in subsets of primary progressive aphasia. *Ann Neurol* 2008;63:709–719.
- Ossenkoppele R, Pijnenburg YA, Perry DC, et al. The behavioural/dysexecutive variant of Alzheimer's disease: clinical, neuroimaging and pathological features. *Brain* 2015;138(Pt 9):2732–2749.
- Dubois B, Feldman HH, Jacova C, et al. Advancing research diagnostic criteria for Alzheimer's disease: the IWG-2 criteria. *Lancet Neurol* 2014;13:614–629.
- Galton CJ, Patterson K, Xuereb JH, Hodges JR. Atypical and typical presentations of Alzheimer's disease: a clinical, neuropsychological, neuroimaging and pathological study of 13 cases. *Brain* 2000;123(Pt 3):484–498.
- Dorothee G, Bottlaender M, Moukari E, et al. Distinct patterns of anti-amyloid-beta antibodies in typical and atypical Alzheimer disease. *Arch Neurol* 2012;69:1181–1185.
- Sahoo A, Bejanin A, Murray ME, et al. TDP-43 and Alzheimer's disease pathologic subtype in non-amnesic Alzheimer's disease dementia. *J Alzheimers Dis* 2018;64:1227–1233.
- van der Flier WM, Pijnenburg YA, Fox NC, Scheltens P. Early-onset versus late-onset Alzheimer's disease: the case of the missing APOE varepsilon4 allele. *Lancet Neurol* 2011;10:280–288.
- Wellington H, Paterson RW, Suarez-Gonzalez A, et al. CSF neurogranin or tau distinguish typical and atypical Alzheimer disease. *Ann Clin Transl Neurol* 2018;5:162–171.
- Whitwell JL, Graff-Radford J, Tosakulwong N, et al. [(18)F]AV-1451 clustering of entorhinal and cortical uptake in Alzheimer's disease. *Ann Neurol* 2018;83:248–257.
- Sander K, Lashley T, Gami P, et al. Characterization of tau positron emission tomography tracer [(18)F]AV-1451 binding to postmortem tissue in Alzheimer's disease, primary tauopathies, and other dementias. *Alzheimers Dement* 2016;12:1116–1124.
- Lowe VJ, Curran G, Fang P, et al. An autoradiographic evaluation of AV-1451 Tau PET in dementia. *Acta Neuropathol Commun* 2016;4:58.
- Marquie M, Normandin MD, Vanderburg CR, et al. Validating novel tau positron emission tomography tracer [F-18]-AV-1451 (T807) on postmortem brain tissue. *Ann Neurol* 2015;78:787–800.
- Lowe VJ, Lundt ES, Albertson SM, et al. Tau-positron emission tomography correlates with neuropathology findings. *Alzheimers Dement* 2020;16:561–571.
- Association AP. Diagnostic and statistical manual of mental disorders, 4th ed. Washington DC: American Psychiatric Association, 1994.
- Crutch SJ, Schott JM, Rabinovici GD, et al. Consensus classification of posterior cortical atrophy. *Alzheimers Dement* 2017;13:870–884.
- Botha H, Duffy JR, Whitwell JL, et al. Classification and clinicoradiologic features of primary progressive aphasia (PPA) and apraxia of speech. *Cortex* 2015;69:220–236.
- Gorno-Tempini ML, Hillis AE, Weintraub S, et al. Classification of primary progressive aphasia and its variants. *Neurology* 2011;76:1006–1014.
- Lowe VJ, Wiste HJ, Senjem ML, et al. Widespread brain tau and its association with ageing, Braak stage and Alzheimer's dementia. *Brain* 2018;141:271–287.
- Jack CR Jr, Lowe VJ, Senjem ML, et al. 11C PiB and structural MRI provide complementary information in imaging of Alzheimer's disease and amnesic mild cognitive impairment. *Brain* 2008;131(Pt 3):665–680.
- Fox J, Friendly M, Monette G. Visualizing hypothesis tests in multivariate linear models: the heplots package for R. *Comput Stat* 2009;24:233–246.
- Neumann M, Sampathu DM, Kwong LK, et al. Ubiquitinated TDP-43 in frontotemporal lobar degeneration and amyotrophic lateral sclerosis. *Science* 2006;314:130–133.

27. Josephs KA, Whitwell JL, Weigand SD, et al. TDP-43 is a key player in the clinical features associated with Alzheimer's disease. *Acta Neuropathol* 2014;127:811–824.
28. Bejanin A, Murray ME, Martin P, et al. Antemortem volume loss mirrors TDP-43 staging in older adults with non-frontotemporal lobar degeneration. *Brain* 2019;142:3621–3635.
29. Josephs KA, Whitwell JL, Tosakulwong N, et al. TAR DNA-binding protein 43 and pathological subtype of Alzheimer's disease impact clinical features. *Ann Neurol* 2015;78:697–709.
30. Nag S, Yu L, Capuano AW, et al. Hippocampal sclerosis and TDP-43 pathology in aging and Alzheimer disease. *Ann Neurol* 2015;77:942–952.
31. Wennberg AM, Whitwell JL, Tosakulwong N, et al. The influence of tau, amyloid, alpha-synuclein, TDP-43, and vascular pathology in clinically normal elderly individuals. *Neurobiol Aging* 2019;77:26–36.
32. Robinson JL, Lee EB, Xie SX, et al. Neurodegenerative disease concomitant proteinopathies are prevalent, age-related and APOE4-associated. *Brain* 2018;141:2181–2193.
33. White L. Brain lesions at autopsy in older Japanese-American men as related to cognitive impairment and dementia in the final years of life: a summary report from the Honolulu-Asia aging study. *J Alzheimers Dis* 2009;18:713–725.
34. Tang-Wai DF, Josephs KA, Boeve BF, et al. Pathologically confirmed corticobasal degeneration presenting with visuospatial dysfunction. *Neurology* 2003;61:1134–1135.
35. Tang-Wai DF, Graff-Radford NR, Boeve BF, et al. Clinical, genetic, and neuropathologic characteristics of posterior cortical atrophy. *Neurology* 2004;63:1168–1174.
36. Akers C, Acosta LMY, Consideine C, et al. Atypical clinical manifestations of cerebral amyloid angiopathy. *Curr Neurol Neurosci Rep* 2019;19:64.
37. Whitwell JL, Dickson DW, Murray ME, et al. Neuroimaging correlates of pathologically defined subtypes of Alzheimer's disease: a case-control study. *Lancet Neurol* 2012;11:868–877.
38. Whitwell JL, Martin P, Graff-Radford J, et al. The role of age on tau PET uptake and gray matter atrophy in atypical Alzheimer's disease. *Alzheimers Dement* 2019;15:675–685.
39. Jones DT, Graff-Radford J, Lowe VJ, et al. Tau, amyloid, and cascading network failure across the Alzheimer's disease spectrum. *Cortex* 2017;97:143–159.
40. Petersen C, Nolan AL, de Paula Franca Resende E, et al. Alzheimer's disease clinical variants show distinct regional patterns of neurofibrillary tangle accumulation. *Acta Neuropathol* 2019;138:597–612.
41. Whitwell JL, Graff-Radford J, Tosakulwong N, et al. Imaging correlations of tau, amyloid, metabolism, and atrophy in typical and atypical Alzheimer's disease. *Alzheimers Dement* 2018;14:1005–1014.
42. Sintini I, Schwarz CG, Martin PR, et al. Regional multimodal relationships between tau, hypometabolism, atrophy, and fractional anisotropy in atypical Alzheimer's disease. *Hum Brain Mapp* 2019;40:1618–1631.
43. Ossenkoppele R, Cohn-Sheehy BI, La Joie R, et al. Atrophy patterns in early clinical stages across distinct phenotypes of Alzheimer's disease. *Hum Brain Mapp* 2015;36:4421–4437.
44. Xia C, Makarets SJ, Caso C, et al. Association of in vivo [18F]AV-1451 tau PET imaging results with cortical atrophy and symptoms in typical and atypical Alzheimer disease. *JAMA Neurol* 2017;74:427–436.
45. Tetzloff KA, Graff-Radford J, Martin PR, et al. Regional distribution, asymmetry, and clinical correlates of tau uptake on [18F]AV-1451 PET in atypical Alzheimer's disease. *J Alzheimers Dis* 2018;62:1713–1724.
46. Ossenkoppele R, Schonhaut DR, Scholl M, et al. Tau PET patterns mirror clinical and neuroanatomical variability in Alzheimer's disease. *Brain* 2016;139(Pt 5):1551–1567.
47. Phillips JS, Das SR, McMillan CT, et al. Tau PET imaging predicts cognition in atypical variants of Alzheimer's disease. *Hum Brain Mapp* 2018;39:691–708.
48. Nasrallah IM, Chen YJ, Hsieh MK, et al. (18)F-Flortaucipir PET/MRI correlations in nonamnesic and amnesic variants of Alzheimer disease. *J Nucl Med* 2018;59:299–306.
49. Johnson KA, Schultz A, Betensky RA, et al. Tau positron emission tomographic imaging in aging and early Alzheimer disease. *Ann Neurol* 2016;79:110–119.
50. Scholl M, Lockhart SN, Schonhaut DR, et al. PET Imaging of tau deposition in the aging human brain. *Neuron* 2016;89:971–982.

Supporting Information

Additional supporting information may be found online in the Supporting Information section at the end of the article.

Table S1. AUROC estimates (95% CI) for differentiating Ty-AD and Aty-AD.

Figure S1. Neocortex minus lateral temporal. We also assessed another neocortical region of interest (ROI) combining the superior, mid, and inferior occipital cortex + lingual cortex + cuneus + calcarine + angular + superior medial and superior lateral frontal cortex + supramarginal cortex + precuneus + superior and inferior parietal cortex from the MCALT atlas.